Chapter 5

Cadmium Zinc Telluride Imager

The Cadmium Zinc Telluride Imager (CZTI) is one among the four X-ray instruments on ASTROSAT. It is a hard X-ray imaging instrument covering the energy band from 10 to 100 keV, has a detector area of 976 cm^2 constructed using CZT modules and uses a Coded Aperture Mask (CAM) for imaging.

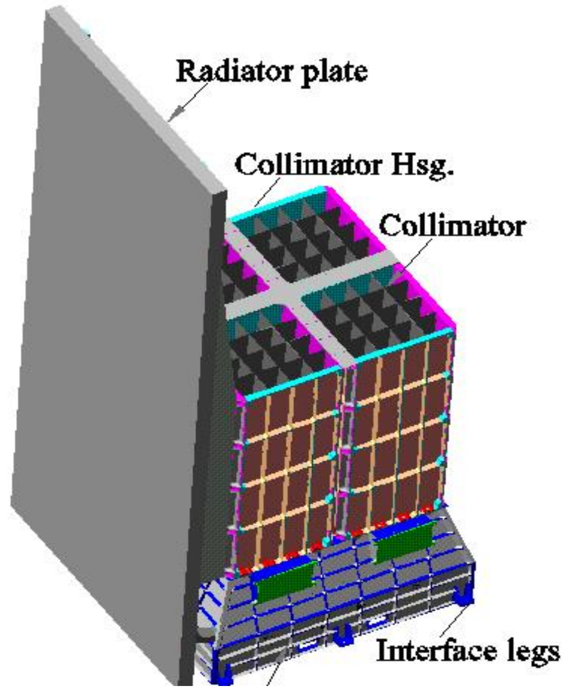

Figure 5.1: The Cadmium Zinc Telluride Imager (CZTI)

The characteristics of the CZT-Imager are given in Table 5.1 (Figure 5.1). The total detection area of 976 cm^2 is achieved by the use of 64 CZT modules of area 15.25 cm^2 each. These 64 modules are arranged in four identical and independent quadrants. The overall dimensions of the CZTI are shown in Figure 5.2 and the orientation reference is shown in Figure 5.3. The CZT detector is interfaced to a radiator plate which maintains an operating temperature of 0 to 15 deg Celsius by passive cooling. The instrument is mounted on the satellite deck with the radiator plate looking in the direction of the satellite +Yaw axis. Collimators above each detector module restrict the Field of View to 4.6° x 4.6° (Full Width at Half Maximum) at photon energies below 100 keV. At energies above that the collimator slats and the coded mask become progressively transparent. For Gamma Ray Bursts, the instrument behaves like an all-sky open detector.

The CZTI carries a Cesium Iodide (Tl) based scintillator detector operated in anti-coincidence with the main CZT detector and it is called the Veto detector. This is located just under the CZT detector modules. Further, there is a gap of about 8 cm between the base of the collimator slats and the detector plane, in order to accommodate a radioactive calibration source module in each quadrant. This source shines alpha-tagged 60 keV photons on the CZT detector in order to help calibrate the energy response.

The science objectives of the CZTI include the measurement of curvature and reflection components in the spectra of Active Galactic Nuclei and X-ray binary systems, the study of Quasi-Periodic Oscillations at hard X-ray bands in accreting neutron star and black hole systems, cyclotron line spectroscopy of high mass X-ray binaries, the characterization of hard X-ray spectra of magnetars as well as the detection of gamma ray bursts and the study of their early light curves. Polarization measurement of gamma-ray bursts and bright (> 500 mCrab) sources in 100 – 300 keV region is an additional objective of CZT Imager.

Table 5.1: Characteristics of the CZT-Imager

Area	976 cm^2
Pixels	16384 (64 modules of 256 pixels each)
Pixel size	2.46 mm X 2.46 mm (5 mm thick); edge row pixels are 2.31 mm wide instead of 2.46 mm
Read-out	ASIC based (2 ASICs per module)
Imaging method	Coded Aperture Mask (CAM)
Field of View (10-100 keV)	4.6^o X 4.6^o FWHM (primary FOV) 11.8^o X 11.8^o FWZM (incl. illumination leakage)
Angular resolution	~ 8 arcmin (18 arcmin geometric)
Energy resolution	~ 6% @ 100 keV
Energy range	10 – 100 keV Up to 1 MeV (Photometric); no imaging above 100 keV
Sensitivity	0.5 mCrab (5 sigma; 10^4 s)
Memory	50 Mbytes per orbit

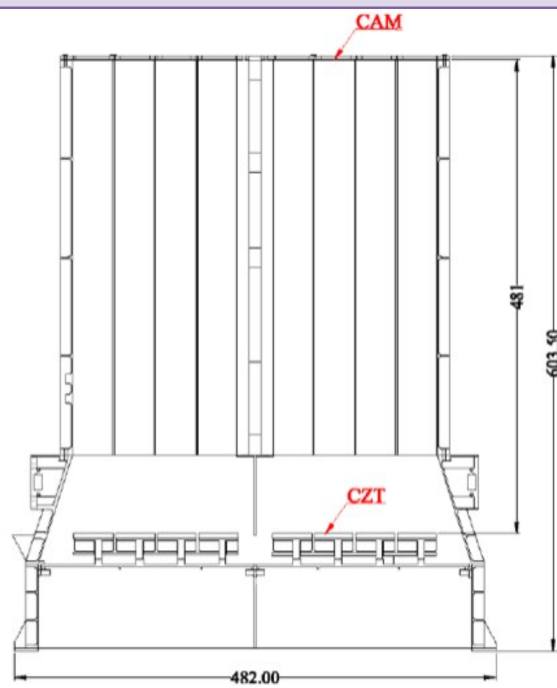

Fig 5.2: Overall Dimensions of the CZT-Imager

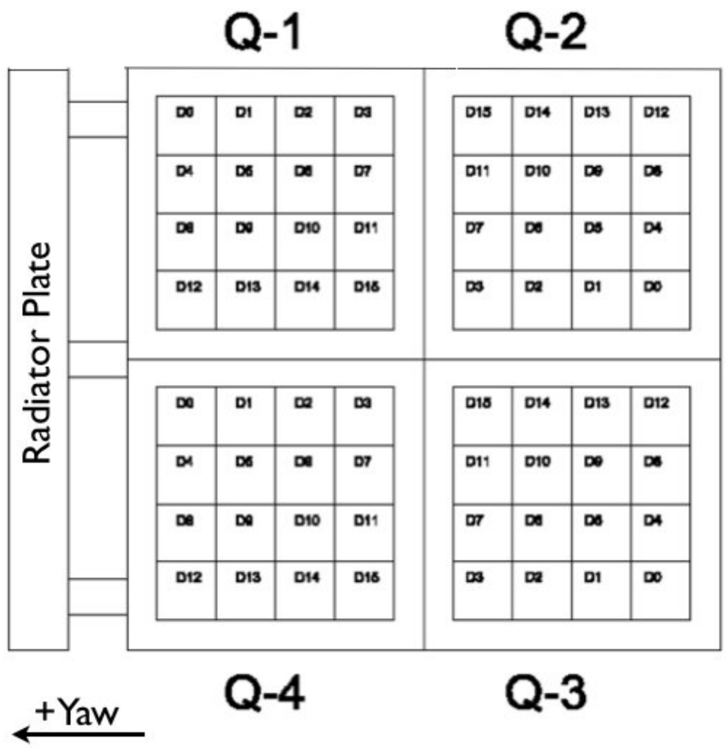

Fig 5.3: Orientation of the CZT-Imager and the reference nomenclature of the four quadrants. The x-axis of the detector plane is identified with the negative Yaw axis of the satellite.

The CZT Imager payload is divided into two packages: CZTI detector box and CZTI Processing Electronics. The detector box houses the detectors with front end electronics and all mechanical interfaces including CAM, cooling arrangement etc. The four quadrants are electrically independent and communicate, digitally, only with the Processing Electronics (PE) box. The PE handles all interfaces (including detector interface) and houses the onboard software designed for the optimum performance of the payload. The basic details of these two packages are given in Table 5.2.

Table 5.2: CZTI Package details

	CZTI Detector Box	CZTI Processing Electronics
Weight (kg)	50	3.2
Size (mm)	482X458 X603	263X256X69
Power (W)	70	3
Operating temperature	0 – 20 °C	0 – 40 °C

Detector Module Details

The CZT-Imager detector box contains Cadmium Zinc Telluride as the main X-ray detector and a CsI (Tl) crystal is used as a veto detector for background reduction. In addition to these two detectors an alpha-tagged X-ray source is also used for calibration purposes (Rao et al. 2010, NIMA, 616, 55). The Front-end electronics in the detector box handles the outputs from these detectors for further analysis while low voltage and high voltage supplies provide the necessary power and biasing voltages to the detectors. A passive collimator (FOV of 4.6° X 4.6° FWHM) helps in allowing nearly parallel X-rays to enter the detector. A Coded Aperture Mask (CAM) made of tantalum is positioned above the collimator.

a. The basic detector module is a CZT crystal of size 39.06 mm X 39.06 mm and 5 mm thick. It is pixelated by contact points on one side with a pixel size of 2.46 mm X 2.46 mm, except for edge rows which are 2.31 mm wide. The edge pixels are thus 2.31mm x 2.46 mm in size, and the corner pixels are of size 2.31 mm X 2.31 mm. One detector module thus becomes an array of 16 X 16 pixels of CZT. The overall geometric area (976 cm^2) of the instrument is achieved by using 64 detector modules divided into four quadrants, each quadrant containing a 4 x 4 matrix of detector modules mounted on the Detector board.

   Each individual pixel is connected to a pre-amplifier, which is embedded in an Application Specific Integrated Circuit (ASIC) containing 128 channels. Two ASICs are situated just behind the detector wafer. The X-ray detector has a detection efficiency of 95% within 10 - 120keV and good energy resolution (~ 6 % at 100 keV). The ASIC is a fully data-driven charge signal acquisition chip. It provides digital output corresponding to the detected X-ray energy and digital address of the incidental pixel.

b. The veto detector is a CsI (Tl) scintillator of size 167 mm X 167 mm and 20 mm thickness viewed by two one inch Photo-multiplier tubes (PMT) positioned on two sides of the crystal. Minimum detection sensitivity is 50 keV for incident photons. The CsI detector requires High Voltage (HV) of the order of 800 V, which is generated by the electronic circuits in the Crystal Holder.

c. Another CsI (Tl) 10 mm cube crystal viewed by a photodiode of 10 mm square area and embedded with a radioactive source Am^{241} is placed on top of the CZT detector. At every disintegration of an Am^{241} nucleus, a 60 keV photon is generated, accompanied by an alpha particle of energy of about 5 MeV. The alpha particle is absorbed in the small CsI (Tl) detector whereas the 60 keV X-rays escape from this detector and in a very substantial number of cases interact in the CZT detector. The alpha particle gives a light pulse in the CsI (Tl) crystal which in turn is converted into an electrical pulse at the output of the photo-diode. Any output in the CZT detector coincident with the pulse output from the CsI (Tl) detector is deemed to be originating from a 60 keV photon. This method is used to calibrate the CZT detector for its energy response.

Mechanical and Thermal Design

The mechanical parts of the CZTI consist of the following:

CZT Imager Housing

The housing is made out of blocks of Aluminum alloy to increase the integrity of the payload. It has an overall dimension of 482 mm x 482 mm x 195 mm height. All peripheral walls (vertical & slant) of the housing are configured with suitable ribs and minimum wall thickness. The top half of the housing has circumferential as well as central flanges which are suitably stiffened by providing gussets and stiffeners to withstand load coming from collimator housing which will be integrated on this.

Crystal Holder

CsI crystal holder is a sub-assembly interfaced with the Detector housing and it accommodates (1) the CsI crystal (2) a Power Card with HV DC-DC, pre-amplifier and power electronics**.** The CsI crystal is mounted on top of the housing and is held by a clamp specially designed for it. The Power card is assembled on the rear side of crystal housing.

Detector Board Assembly

The Detector Board consists of a PCB to mount the 16 detector modules, Front-end Electronics Board (FEB), and a specially designed Internal Radiator Plate which acts as an interface between the detector modules and the heat pipes so that uniform temperature is maintained across all detector modules.

Functions of detector board assembly:

- Holding the CZT detector modules in a specified format.
- Providing interface to the Detector housing.
- Providing interface to the Calibration housing.
- Providing interface to the heat pipes.

Radiator Assembly

The CZT modules perform best in a temperature range of 0° C to 15° C. To achieve this temperature, the heat produced by CZT module (300 mW/module) is drained continuously by the radiator assembly, which consists of (i) Heat pipes (3 nos.) (ii) Radiator plate and (iii) Spacers & clamps. The radiator plate area required to radiate the total power of 50 W is about 7000 cm^2.

Collimator

The Collimator plates are made of 0.07 mm thick Tantalum sheet sandwiched between 0.2 mm thick precisely machined Aluminium alloy plates, providing a collimation of 4.6° X 4.6° FWHM directly under the collimator. However since a gap of 100 mm is left between the bottom of the collimator and the detector plane to accommodate the calibration housing, a certain amount of illumination leakage occurs from one collimated module to its adjacent neighbours. When this illumination overlap is taken into account, the net field of view works out to be 11.8° x 11.8° FWZM.

Collimator housing

The Collimator housing is a hollow structure, configured quadrant wise, with a single quadrant 167.5 mm x 167.5 mm x 400 mm, made up of four aluminum alloy side plates, which are integrated side-by-side using M4 fasteners.

The Coded Aperture Mask

The design of the CAM for the CZTI is such that the size of the mask plate is the same as that of the detector itself. The mask is made of a 0.5 mm thick Tantalum plate in which a pre-determined pattern of holes is cut to allow X-rays to pass through. The Coded Mask forms the topmost part of CZTI payload. It is coded by open and closed pattern of squares/rectangles matching the size of the detector pixels. Additional support bridges of thickness 0.2 mm are introduced at a number of places within the pattern to improve its mechanical stability. In such a design (called a 'box-type' or 'simple' system) exposure to the full mask pattern is not possible anywhere except exactly at the middle of the coded field of view. At all other angles only a part of the shadow of the mask falls on the detector. The patterns are based on 255-element pseudo-noise Hadamard Set Uniformly Redundant Arrays. Of sixteen possible such patterns, seven were chosen on the basis of the mechanical support for individual pixels in the pattern. These seven patterns, with some repeats, were placed in the form of a 4 x 4 matrix to generate the CAM for one quadrant. This same pattern is placed on other quadrants, rotated by 90°, 180° and 270° respectively.

CZTI Detector Electronics

The CZT detector box electronics consists of

1. The front end electronics for CZT module.
2. Pre and Post amplifiers for Veto detector Cesium Iodide {CsI (Na)}.
3. Pulse height (PH) analyzer for Veto.
4. Alpha source detector CsI (Na).
5. Logic circuits to handle the data.
6. The high voltage DC/DC converters.
7. Interface circuitry for communication with CZTI Processing Electronics.

The front-end electronics is made into four identical quadrants. All analog electronics is housed in the detector box itself and it contains ASIC control, amplifiers etc. Apart from Detector Board, Alpha card and the Power Card, there will be one electronics card per quadrant called the FEB which includes ADCs, digital control and FPGA.

Basic Design

One CZT module contains 2 ASICs and hence one quadrant will have 32 ASICs daisy chained to each other. A list of major components of CZT Detector electronics is given in Table 5.3. The detector assembly consists of the array of Detector Modules which is an integrated unit of CZT detector and ASICs, procured from Orbotech Medical Solutions, Israel. The detector assembly contains a Detector Board with 16 CZT Modules with 32 ASICs daisy chained. An aluminized Mylar sheet of 50 micron thickness is kept on top of the detectors to provide thermal isolation.

Table 5.3 List of Major Components of CZT-Imager Quadrant

Name	Components	Mechanical Location
CZT Detector Assembly	Detector Modules Detector Board Internal Radiator FEB	Detector Board Assembly
HV-CZT	Pico DC/DC	Detector Board Assembly
Veto Detector	CsI(Tl) + 2 PMTs	CsI Assembly
HV-Veto	HV DC/DC (800V)	CsI Assembly
Alpha Tag	Am (241)	Alpha-Box

Veto Detector

A detector (CsI) covers the large area of 256 cm^2 and the light collection is done using two photomultipliers (PMT), viewed from sides. On registering an event, a signal from the detector is sent to a pre-amplifier. This signal is processed and sent to the FEB for further analysis. After amplification of the signal from pre-amplifier, the signal is sent to a comparator via stretcher along with LLD level signal. If LLD is triggered the pulse is digitized to an 8-bit output by ADC through control circuit. This output is used to differentiate Compton scattered events and hence the background in main detector can be reduced.

Power Card

The Power card, positioned in the Crystal Holder, has a Pico high voltage generator for biasing the veto detector. A positive high voltage around 800 V is used to bias the Photomultiplier tubes attached to Veto detector. Similarly another negative high voltage, from another Pico DC/DC converter, is used to bias the CZT detector. The Power Card also generates appropriate regulated low voltages for the CZT modules and it also houses the amplifiers for the CsI detector.

Alpha - Tag

A calibration source of Am (241), is kept to shine over the detector. An energy of 60 keV is released from the source along with an alpha particle simultaneously. This alpha particle gets detected in the CsI (Tl) detector volume which generates the signal. The photodiode which is coupled to this CsI (Tl) detector generates an electrical pulse, which is amplified in pre-amplifier and post-amplifiers. Post-amplifier signal is fed to an analog comparator along with lower-level discriminator level. A relevant digitized signal generated with help of Monoshot is passed on to FPGA as an alpha-tag event.

Front-end Electronics Board (FEB)

The FEB contains interface circuits required for the CZT modules. A FPGA is used to handle the signals from the three different detectors (CZT, Alpha and CsI Veto) and data is stored in a memory to be transmitted to PE, every second. The coincidence among different detectors are done digitally by ground data processing.

Processing electronics

The Processing Electronics (PE) is housed separately and it contains an FPGA with an embedded processor. The PE controls all satellite interfaces, detector interfaces and it handles onboard memory and data management. The functions of the processing electronics includes reading, analyzing, storing and/or transferring detector data to satellite via data formatter. Also it controls the FPGA in the FEB using 16-bit serial commands.

There are two types of memories, namely

a. RAM: This holds all types of data like detector data and commands, telecommands and telemetry data.
c. EEPROM: This holds the basic software and the default parameters. Initially all parameters are copied from EEPROM and then any changes sent by telecommands are stored only in the RAM.

About FPGA: this is mainly a hardware compressor, in that it compresses the overall hardware into one single chip. This handles the following functions:

a. Timer.
b. Detector communications.
c. Telecommands.

During an event in the detector package, the same is analyzed and stored in one of its ping-pong memory, by its FPGA. The CPU interrogates the detector FPGA every 1 second. Upon receiving this signal the FPGA stops storage in the first of its ping-pong memory, resumes storage of data in the second memory and, upon command from the CPU, transfers data from the first memory to processing electronics. This FPGA based data are stored directly into a pre-determined space in the CPU memory. Data from all the 4 quadrants are read simultaneously (the entire data transfer at 500 kHz takes about 131 ms). The CPU then starts analyzing the stored data according to its operating mode.

Data Organization in Detector Package
The detector package contains a FPGA to analyze data from ASICs, store it in its RAM and send it to the electronics package. All the ASICs are daisy chained hence the inputs and outputs of all 32 ASICs in a quadrant are controlled by a single FEB.

Modes of Operation

The CZTI can operate in 16 possible modes. Fifteen of these are primary modes, and there is one Secondary Spectral Mode which runs in parallel with other primary modes. The description of these modes are as follows:

Normal Mode:
This mode transmits complete raw data received from the detector box. This takes up 144 Mbytes per 100-minute orbit. This is the default mode of operation of the CZTI.

SAA Mode:
When the detector is in the South Atlantic Anomaly (SAA), or if both the CZT and the Veto High Voltage supplies have been turned off by ground command, only header data is transmitted directly from the event frame. The header data of each second is extracted and compiled into one quadrant header packet every 100 seconds.

Shadow Mode:
The Shadow Mode is selected if the Earth Shadow Entry command is sent from ground. In this mode the header data of a 100-s window is sent at the 100-s boundary. The Frame/packet format is similar to the SAA mode. Each frame contains only one packet.

Secondary Spectral Mode:
This mode runs in parallel with any other selected mode. The on-board software prepares the spectral data of each quadrant every second. The integrated spectra so prepared is packetized and sent to the Satellite Bus storage (Solid State Recorder) once every 100 seconds.

Reduced Data Modes
Reduced Data Modes can be entered either by ground command or due to limited memory availability. The following reduced modes of operation are available:

Fixed No. of Packets (FP):
The frame format here is similar to the normal mode but a fixed maximum number of packets are generated from each quadrant.

Veto Spectrum Disabled (VSD):
Packets are generated without the Veto Spectrum.

Two word event report (2WE):
The number of words representing each event is reduced from 3 (as in normal mode) to 2, by sacrificing some resolution in time and energy.

Memory Management (MM):
The behavior of Memory Managed modes depends on the level to which the payload memory is occupied due to the Satellite Bus storage allocated to the CZTI being full. At different levels, Full data, only Secondary Spectral Mode data and Header data or the Header data alone could be recorded. Beyond a certain level no data is recorded.

A number of combinations of the reduced modes are possible, e.g., SAA+Shadow, VSD+2WE, VSD+FP, FP+2WE, FP+2WE+VSD, MM+SAA, MM+Shadow and MM+Shadow+SAA.

Data Interfaces

The two main interfaces are namely:
1) Detector Interface.
2) Satellite Interface.

Detector Interfaces:

The unit's interface with the detector electronics unit involves the following:

Event Interface:
The FPGA of each quadrant reads data from the detectors, arranges it in the form of a 2 x 2 Kbytes frames This is read periodically by the processing electronics every 1 second. This data is then further analyzed and accumulated or transmitted to the satellite via data formatter.

Command Interface:
The Command interface with the detector unit is done serially with clock & data lines.

Satellite Interfaces:

The unit's interface with the satellite involves the following:

Power Interface:
The raw power is routed through a relay, which is switched ON/OFF by command from ground followed by a series of transfers to the motherboard. There are two separate lines for main & redundant power.

Command Interface:
There are 13 Pulse commands & one 32-bit data command with the facility of sending data commands in a time-tagged mode.

Telemetry Interface:
This interface is to a Solid State Recorder (SSR) via a data formatter. Data is sent periodically, typically every 8 ms, to the formatter in the form of 2 Kbytes frame at 2MHz clock rate.

Background Estimation

The sources of background in the CZT detector are primarily cosmic diffuse gamma rays and gamma-rays originating from the satellite structure (spallation background) due to the interaction of cosmic rays.

To distinguish these background counts from the real source counts a slab of CsI is placed under each block of CZT. The high energy photons which deposit energy in CsI as well as CZT are rejected by anti coincidence techniques and hence do not contribute to the background counts in CZT. Only the photons which deposit partial energy in CZT but do not interact in the CsI block generate background counts in the (10 - 100) keV region.

Compton Induced Background

Assuming an outer space environment where the satellite is deployed, some of the background count estimates have been simulated and the values are described here. The total number of background counts in the CZT due to single Compton scattering are calculated by summing up all the contributions over the entire energy range of injected gamma rays and the typical counts are about 20 counts/sec for CsI thickness of 2 cm.

Fluorescent K-alpha Background

Cosmic diffuse gamma ray photons in the energy range (10 - 100) keV interacts with Tantalum by photo-electric effect and produce fluorescent Kα X-rays. The fluorescent X-ray contribution to background contributions can be divided in 3 parts:

(a) Contribution from the top surface,

This surface is made up of Tantalum of thickness 0.5 mm. The total area of a module is 15.25 cm^2 but the effective area is half that due to the random holes of the CAM. It is far from the detector and subtends a small solid angle at the detector plane. The total counts from this surface are about 0.0025 counts / sec.

(b) Contribution from 4 cm x 36 cm upper side surfaces.

This side is made of Tantalum sheet of area 4 cm x 36 cm and thickness 0.1 mm. Though this surface is large compared to the detector surface, it is perpendicular to detector plane and makes a small solid angle to the detector. The total count from this surface is about 0.41 counts / sec.

(c) Contribution from 20 cm x 14 cm lower side surfaces.

This is the lower portion of the side surface and as it is closer to the detector it contributes the maximum. The numbers of counts at the detector depends very much on the height of the side surface. The total counts from this surface are about 5 counts/sec.

Data Analysis

Image Reconstruction

The standard procedure adopted for image reconstruction will consist of first binning the data to produce a detector plane image (DPI), which is then cross correlated with the mask pattern. Significant peaks from this image are picked and a least square fit is then made of the DPI with theoretically computed shadow patterns for sources these locations. This allows accurate determination of the intensities of these sources, and also helps identify and eliminate spurious peaks that might have been picked from the cross-correlated image.

Operation Sequence to generate the Data products

- Step 1: Download telemetry data for an observation period.
- Step 2: The good time interval file is generated using the house keeping information
- Step 3: Read the attitude information and generate average position of the satellite for the period of observation.
- Step 4: Extract the relevant data and generate the raw DPH or raw DPI.

- Step 5: The detector data (DPH) is processed to generate information about noisy and dead pixels for the time of observation.
- Step 6: Using information generated in steps 3 and 5, process the raw DPH/ DPI and clean them. Generate a detector mask file that records the pixels removed in the cleaning process.
- Step 7: Perform cross-correlation imaging and pick candidate sources from the image
- Step 8: Perform shadow fitting to estimate fluxes of candidate sources, reject insignificant candidates and iterate until all sources have fitted flux values above the detection threshold. (In generating shadow patterns for fitting the detector mask must be accounted for).

Ground Calibration of CZT Imager

The CZT detector modules, procured from Orbotech Medical Solutions, are meant for commercial use. To qualify these detectors for flight, a rigorous screening procedure was evolved. After the screening process, it was found that the yield was very low (about 65%). It was noticed that the number of noisy pixels increased after screening, resulting in the rejection of a large number of modules (acceptance criterion is that the number of dead+noisy+bad pixels out of the 256 pixels in a given detector should be less than 15). The CZT detector modules are primarily designed as gamma-ray devices (40 – 200 keV) to be operated at room temperatures. To extend the low energy response to 10 keV, the devices are cooled to 10°C (+/- 5°C) – but in some orbits the temperature can go up to 20°C.

The ground calibration of CZT-Imager payload was done in the following manner. Time tagging and polarization abilities are examined at individual module level. The assembled quadrants are calibrated at multiple temperatures to understand the spectral response at individual pixel level. The fully assembled payload is calibrated to understand the a) imaging behavior, b) veto tagging efficiency and c) alpha-tagging efficiency.

Characterization of individual pixels

Individual pixels are characterized as dead (D) pixels defined as pixels having no sensitivity to detect X-rays, noisy (N) pixels defined as pixels having counts more than 5-sigma above the mean and bad (B) pixels defined as pixels whose energy resolution is significantly worse as compared to the other pixels. The characteristics of the pixels are monitored regularly and each module is given a grade based on the number of dead and noisy pixels and their degradation with time, based on the criterion given in Table 5.3. The distribution of the grades of 64 modules in the individual quadrants are given in Table 5.4 and it is found that 84% of the modules belong to Very Good or Good category. Noise is also found to be a function of temperature and energy threshold and the final energy threshold that can be achieved at various temperatures are given in Table 5.5 and the number of suppressed pixels are given in Table 5.6. It is found that a threshold of 10 – 15 keV can be achieved in a majority of modules with less than 5% of pixels being suppressed.

Table 5.3 Module grading criterion

	D+N = 0-10	D+N = 11-15	D+N = 16-20	D+N = 21+

Change <= 5	Very Good	Good	Fair	Poor
Change = 6-10	Good	Fair	Poor	Poor
Change >10	--	Poor	Poor	Poor

Table 5.4 Distribution of module grades

	Very Good	Good	Fair	Poor
Quadrant 1	12	3	1	0
Quadrant 2	14	1	1	0
Quadrant 3	10	2	1	3
Quadrant 4	10	2	2	2
Total	46	8	5	5

Table 5.5 Number of modules as a function of threshold for different temperatures.

Temperature (°C)	**Threshold**				
	10 keV	**11-15 keV**	**16-20 keV**	**21-30 keV**	**>30 keV**
-5	38 (59%)	20 (31%)	5 (8%)	1 (2%)	--
0	34 (53%)	19 (30%)	10 (15%)	1 (2%)	--
5	33 (52%)	17 (26%)	13 (20%)	1 (2%)	--
10	31 (48%)	16 (25%)	14 (22%)	3 (5%)	--
15	24 (38%)	8 (12%)	16 (25%)	9 (14%)	7 (10%)
20	--	--	21 (33%)	30 (47%)	13 (20%)
25	--	--	--	--	64 (100%)

Table 5.6 Number of disabled pixels

Temperature	**Number**						
	-5°C	**0°C**	**5°C**	**10°C**	**15°C**	**20°C**	**25°C**
Quadrant 1	100	100	102	111	131	139	152
Quadrant 2	76	78	81	93	110	126	142
Quadrant 3	129	136	143	162	176	185	199
Quadrant 4	148	152	158	170	183	198	224
Total	453 (3%)	466 (3%)	484 (3%)	536 (3%)	600 (4%)	648 (4%)	717 (4%)

X-ray spectroscopic calibration at various temperatures

Calibration data were obtained by shining various radioactive sources (^{241}Am, ^{57}Co and ^{109}Cd) on the quadrants at various temperatures. For automatic analysis, monochromatic lines are modeled as a Gaussian in a region around the peak (−1σ' to +2σ' of the channel with highest counts, where σ' is the approximate Gaussian σ). The mapping between ADC channels and energy (keV) is given by,

$$Energy = Channels \times Gain + Offset$$

Gains and offsets measured for all pixels at different temperatures. A typical energy spectrum is shown in Figure 5.4. In most detector modules, inter-pixel gain variations are small (< 10%). The typical energy resolution is shown in Figure 5.5. The energy resolution at 22 keV and 33 keV are likely to be overestimates because the line blends at these energies are not segregated. There is a marginal change in gain and energy resolution as a function of temperature in 0 – 15 keV region. For onboard response calculation, however, the measured gain and spectral response at each temperature will be used.

Figure 5.4 Spectra for different energies

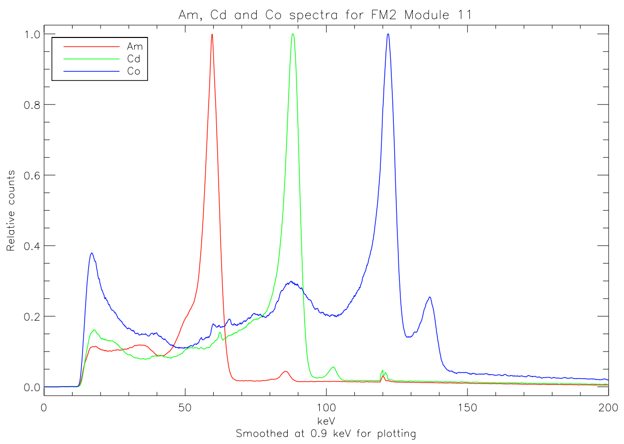

Fig 5.5 Energy resolution as a function of energy

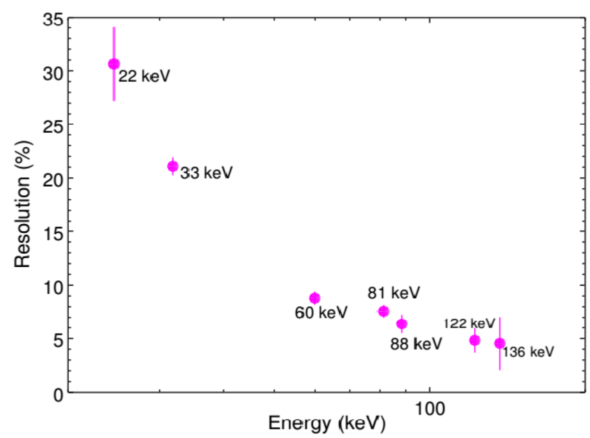

Coded Aperture Mask (CAM) Calibration

The shadow patterns of the CAM and the coding techniques are tested to check the efficiency of the coding device to the given radiation. This is done by shining strong radioactive sources at known fixed positions, typically 100 – 200 cm above the mask. The radiation from the source, on its way to the CZT detector, was intercepted by the coded mask plate situated at a height of 48 cm above the detector. The photons detected by the CZT module were accumulated into an event list, recording the position (pixel number), energy (PHA channel number) and time of each event plane. These data were then analysed using the CZTI imaging algorithm and the location of the source thus reconstructed was compared with the position at which the radioactive source was placed during the acquisition of the data. The reconstruction process began by counting the total number of events recorded in each detector pixel, resulting in a Detector Plane Histogram (DPH). Each count value in the DPH was then divided by the relative quantum efficiency of the corresponding pixel. The array resulting from this is called a Detector Plane Image (DPI). This DPI is a linear combination of shadows of the coded mask cast on the detector plane by sources in the field of view. A library of shadow patterns expected from sources located at different positions on the source plane was created by a ray tracing method. Different methods like Cross correlation, chi-square shadow fitting, and Richardson-Lucy algorithm (based on Bayesian inference), were applied to get the source position. It was found that results from the three different methods agree well, to better than 2 arcmin. The test was repeated at two different energies (60 keV and 122 keV) and it was found that at 122 keV, the PSF is seen to widen slightly, by about 10%. Above 100 keV the mask plate begins to become transparent, reducing shadow contrast and worsening the imaging capability. The results, however, show that decent imaging would still be possible at energies as high as 120 keV, with a PSF of less than ~4 arcmin FWHM.

Field of View of the CZT imager

The Field of View (FoV) of the CZT imager is energy dependent due to greater transparency of the collimator material at higher photon energies. The angular response pattern contains a central core of ~6 deg radius which is common to all energies, and represents the view through the top coded mask surface. Transmission through the collimator slats and side walls contribute wings to the response pattern, the relative strength of which rises with increasing energy. The FoV may therefore be quantified as the amount of solid angle the response pattern covers at a given fraction of the peak on-axis response. It is to be noted that not all of this coverage may be contiguous. We compute the FoV by summing the solid angle of all parts of the effective area distribution that rise above a specified fraction of the on-axis value. The resulting estimates, for different photon energies, are presented in the Fig. 5.6. The FoV evaluated at 50%, 20% and 10% of the peak response at each energy is shown. The FoV increases monotonically with photon energy, apart from a bump near 67 keV due to Tantalum K escape.

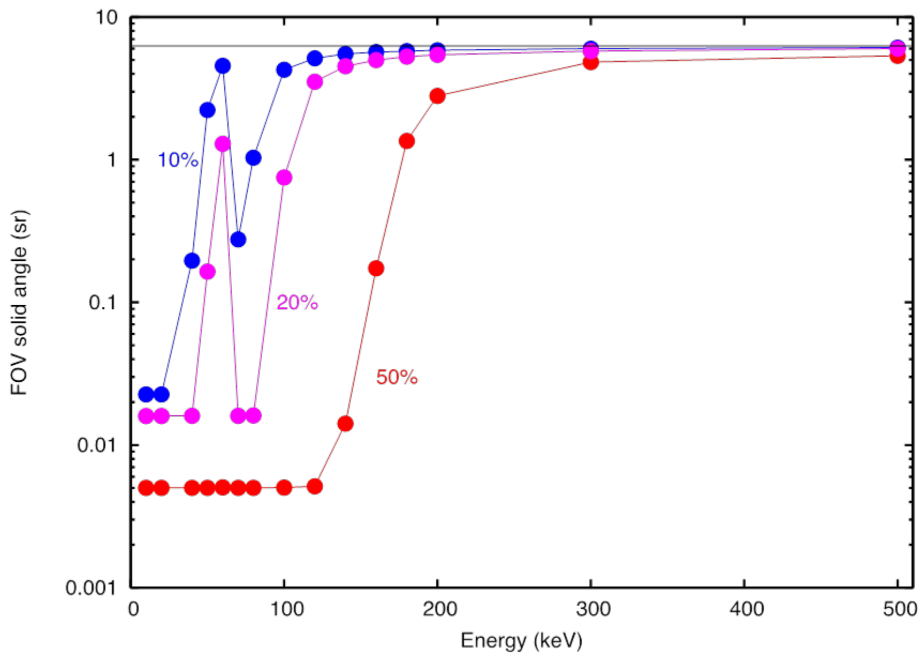

Fig. 5.6 Field of View of the CZT Imager as a function of energy

Effective Area of the CZT Imager

The effective area of the CZT Imager as a function of photon energy and illumination angle has been estimated by accounting for the energy-dependent transmission through the various surfaces making up the CZTI structure, and the energy-dependent absorption by the CZT detector, at different angles of incidence. The result is shown in Fig. 5.7 below. The local peak in effective area near 67 keV occurs due to Tantalum K escape.

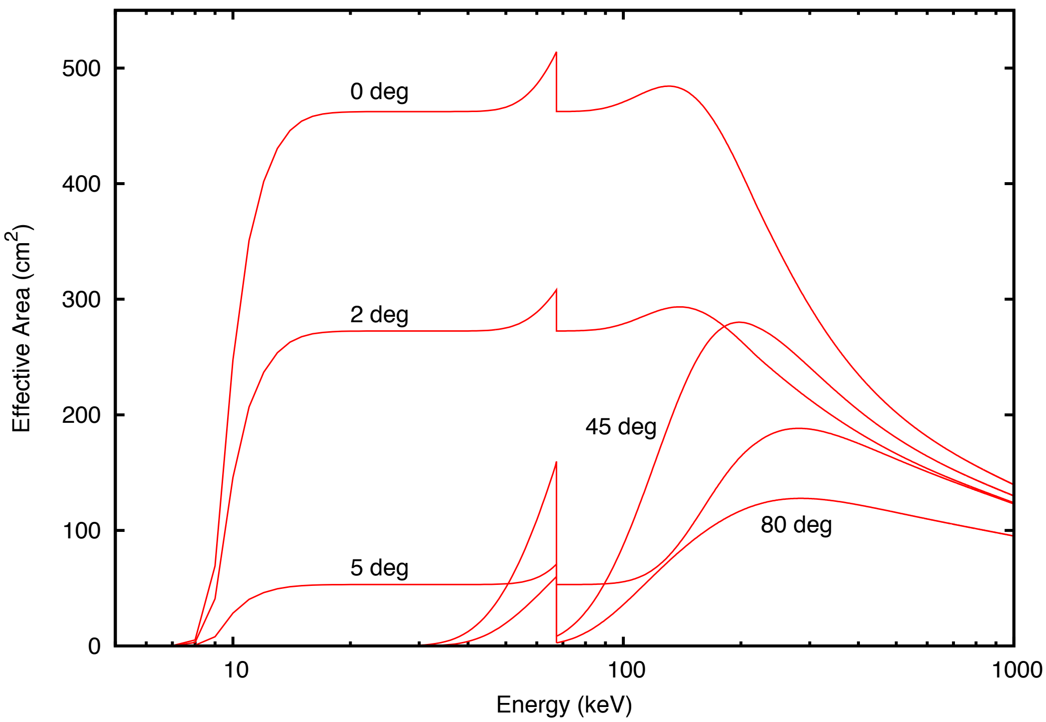

Fig. 5.7: Effective area as a function of energy of the Astrosat CZT Imager at normal incidence (0 deg) and several other off-axis angles.

Alpha-tagging in CZTI

A 10 mm^3 CsI(Tl) crystal, embedded with a radioactive source ^{241}Am and viewed by a photodiode of 10 mm^2 area, is placed beside the CZT detector. With each disintegration of the 60 keV photon from this source, an Alpha particle (energy about 5 MeV) is also emitted. The alpha particle is absorbed in the small CsI(Tl) detector, whereas the 60 keV X-rays will escape from this detector and, in most cases, will interact with the CZT detector. The alpha particle produces a light pulse in the CsI(Tl) crystal, which in turn is converted into an electrical pulse at the output of the photo-diode. Any output in the CZT detector coincident with the pulse output from the CsI(Tl) detector is deemed to be originating from a 60 keV photon. This method is used to calibrate the energy response of the CZT detector for its energy response. The basic design principles are discussed in Rao et al. (2010, NIMPA. 616, 55) and it was estimated that, for an alpha source strength of 1000/s, about 20 – 30 60 keV X-rays should be emerging from the alpha module. The time co-incidence was done digitally and this aspect is rigorously tested in the QM and one FM detector. The tunable parameters were examined carefully, and it was found that the alpha-tagged information can indeed be extracted from the data. However, the flight configuration is such that the final alpha count rate is as low as ~1 count/s, necessitating a large integration time, grouping of pixels, and use of background lines for the onboard calibration.

Veto calibration

The veto detector is a 20 mm thick CsI(Tl) scintillation, of size 167 mm X 167 mm, viewed by two one inch Photo-multiplier tubes (PMT) positioned at two sides of the crystal. Minimum detection sensitivity is 50 keV for incident photons. The main purpose of this detector is to recognize background X-ray/ gamma-ray radiation (above 100 keV) and tag the main X-ray events (in the CZT detector) with the information that the X-rays are accompanied by a background X-ray/ gamma-ray. The energy resolution of this detector is not significant. These detectors are procured from Scionix Holland, the same suppliers who have provided the RT-2 phoswich detectors and the ACS system for Chandrayaan-I. For the CZT-Imager, it was decided to carry out a minimum screening of 10 cycles of thermo-vac cycling (passive). The temperature range was -20 to +50° C. The HV parts were potted with HV 93-500 and the screening and thermo-vac tests were done after the potting. It was found that the gain uniformity over the area is correct to 10%. After the FM assemblies, the amplifier gain was adjusted so that the upper level corresponds to about 500 – 600 keV. The LLD, however, can be changed by command. The test results show that the peak position is linear with energy.

The Veto detector is designed to capture the forward scattered gamma-rays. In the laboratory, it is quite difficult to reproduce this result because any gamma-ray source, like ^{133}Ba, has a low energy line with much higher probability of interaction. It was, however, possible to capture the Compton scattered events by restricting the energy range of CZT detectors to a narrow window of 40 – 70 keV (to detect only the Compton scattered events). When plotted against the coincidence window time, at > 12 micro-seconds, the data shows the expected coincidence events (about 10% of the total events).

Time tagging and polarization

In CZT-Imager, individual photons are tagged to an accuracy of 20 micro-seconds. The onboard clock is logged every 16 seconds based on a pulse coming from the Satellite Positioning System (SPS) and ground calibrations show that the PE time can be correlated to SPS time correct to about 2 microsec. The pixilated nature of the detector can be used for measuring the polarization of the incident X-ray photons based on the principle of Compton scattering by detecting the Compton scattering event in one pixel and the scattered photon in another pixel. However this requires the capability of recording two simultaneous events in different pixels. This polarization ability of CZT modules are verified in the laboratory. Details of this experiment is given in Vadawale et al. (2015; A&A submitted) and in Fig 5.8 we show the fitted and the experimentally observed modulation patterns demonstrating that CZT-Imager is capable of measuring polarization of bright onboard sources (> 500 mCrab) in the 100 – 300 keV region.

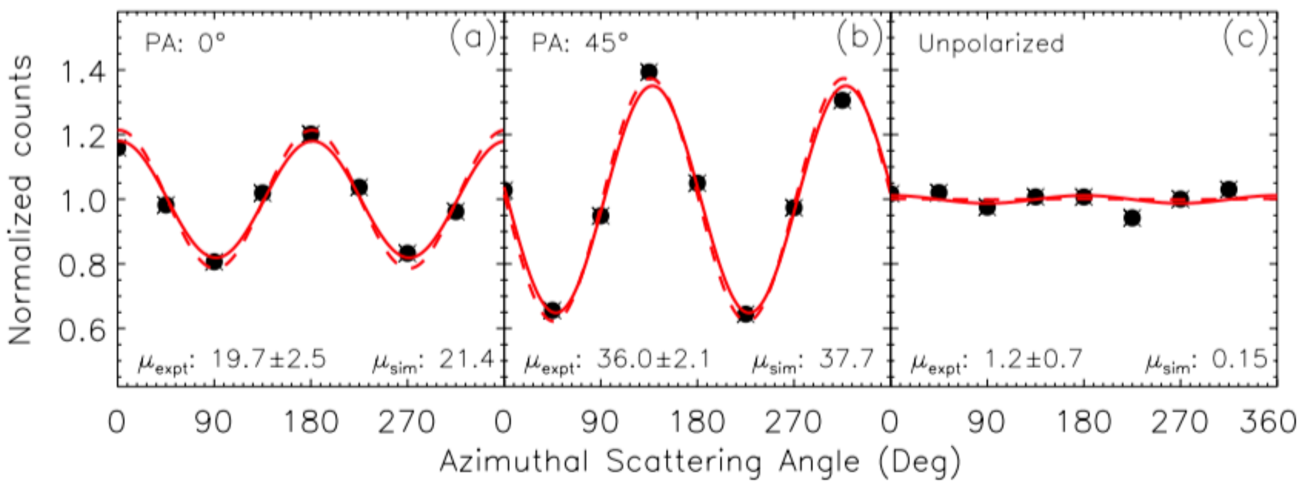

Fig 5.8: Experimentally measured modulation curves for partially polarized X-rays at two polarization angles.

Response matrix generation

Mono-energetic lines detected by CZT detectors have a long tail toward low-energies originating from the partial charge collection due to 'hole-trapping'. This is modeled in terms of crystal charge transport properties. CZT detector line profile and its dependence on the basic parameter is well understood and the model is implemented in IDL, S-Lang (available in ISIS as a local model) and the 'mobility lifetime' products for charge carriers are obtained by simultaneous fit to individual pixel spectra at multiple energies. Sufficient calibration data are available to generate pixel wise parameters at multiple temperatures (gain, offset, resolution, and other line parameters) and a flow chart is given below.

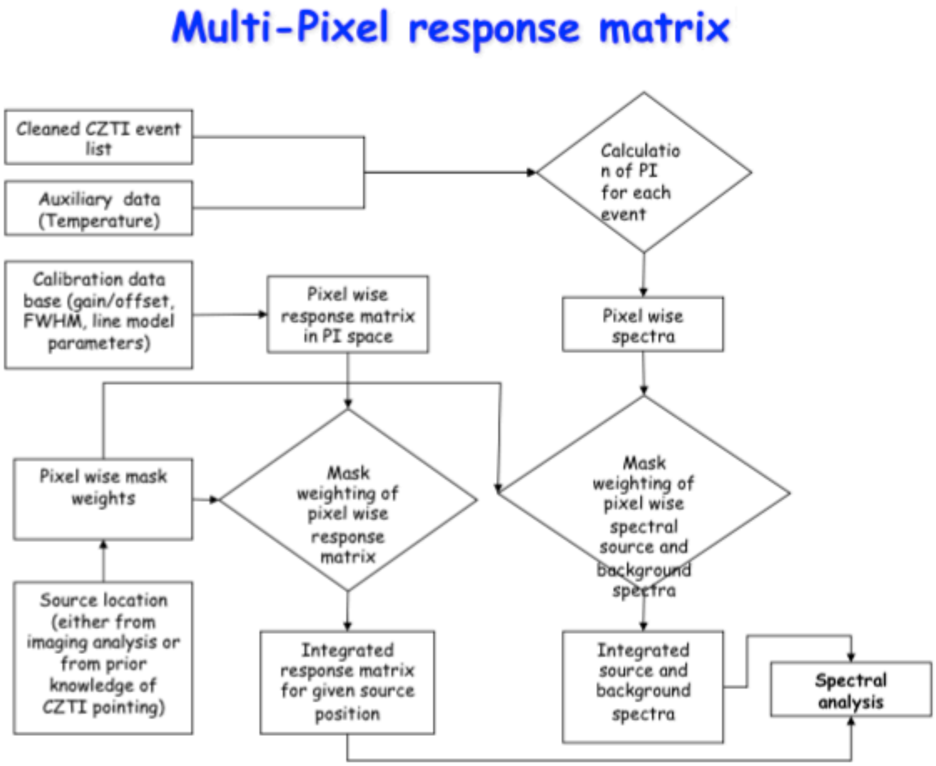

Figure 5.9: Flow-chart for multi-pixel response matrix generation